scientific reports

Check for updates

OPEN

Brain diffusion tensor imaging changes linked to the split hand phenomenon in amyotrophic lateral sclerosis

Seol-Hee Baek[1], Woo-Suk Tae[2,7]✉, Dorothee Auer[3,4,5] & Byung-Jo Kim[1,2,6,7]✉

The split-hand phenomenon is an early and specific feature of amyotrophic lateral sclerosis (ALS). This study aimed to investigate whether the split-hand phenomenon in ALS is associated with the white matter degeneration of the brain. Patients diagnosed with clinically definite or probable ALS were prospectively recruited and underwent both nerve conduction studies to assess the split-hand index (SHI) and brain diffusion tensor imaging (DTI). Demographic, clinical, and electrophysiological data were all collected. A total of 35 patients with ALS (18 male; median age, 66.0 years) were enrolled in this study. The axial diffusivity (AD) and mode of anisotropy (MO) values of DTI in the corticospinal tract (CST) positively correlated with the SHI. However, there were no significant correlations between the SHI and the fraction anisotropy (FA), mean diffusivity (MD), and radial diffusivity (RD) scalars. In addition, patients having ALS with bilateral split-hand phenomenon showed reduced AD values in the left CST and reduced MO values in the bilateral CST compared with those without the split-hand phenomenon. However, there were no significant differences in FA, MD, and RD scalars. Our findings suggest that the split-hand phenomenon is associated with degenerative brain changes, particularly in the CST.

Keywords Amyotrophic lateral sclerosis, Split-hand phenomenon, Pathophysiology, Corticospinal tract, Diffusion tensor imaging, Axonal degeneration

The split-hand phenomenon, observed in patients with amyotrophic lateral sclerosis (ALS), is characterized by a dissociative hand muscle atrophy pattern, predominantly affecting the muscles on the lateral side of the hand (thenar & the first dorsal interosseous muscles), while the muscles on the medial side (hypothenar muscles) are relatively preserved[1]. This phenomenon is recognized as an early and specific clinical feature, and is considered a potential diagnostic biomarker of ALS[2]. Menon et al. previously proposed the split-hand index (SHI), calculated by multiplying the compound muscle action potential (CMAP) amplitude of the abductor pollicis brevis (APB) muscle by that of the first dorsal interosseous (FDI) muscle, and dividing by the CMAP amplitude of the abductor digiti minimi (ADM) muscle[3]. Furthermore, several previous studies using the motor unit number estimate, motor unit number index, and muscle ultrasound, have demonstrated that SHI could be a potential diagnostic biomarker of ALS[4–6]. Indeed, one recent meta-analysis pooling the results of 17 studies with a total of 1,635 patients with ALS reported that an SHI value of < 7.4 has potential as a diagnostic biomarker for distinguishing early-stage ALS from normal controls, with a 75.3% sensitivity and 75.4% specificity[7]. These findings suggest that the split-hand phenomenon could be a distinctive feature of ALS, as well as a useful diagnostic biomarker for ALS.

Despite its prominence as a diagnostic biomarker for ALS, the pathophysiology of the split-hand phenomenon is not fully understood. Several pathophysiological hypotheses have been proposed, including cortical dysfunction, spinal motoneuron dysfunction, peripheral nerve excitability, and neuromuscular junction

[1]Department of Neurology, Korea University Anam Hospital, Korea University College of Medicine, 73, Goryeodae-ro, Seongbuk-gu, Seoul 02841, Republic of Korea. [2]Brain Convergence Research Center, Korea University College of Medicine, 73, Goryeodae-ro, Seongbuk-gu, Seoul 02841, Republic of Korea. [3]Division of Mental Health and Clinical Neuroscience, School of Medicine, University of Nottingham, Nottingham NG7 2UH, UK. [4]Sir Peter Mansfield Imaging Center, School of Medicine, University of Nottingham, Nottingham NG7 2UH, UK. [5]Nottingham Biomedical Research Center, National Institute for Health Research, Queens Medical Center, Nottingham NG7 2UH, UK. [6]BK21 FOUR Program in Learning Health Systems, Korea University, Seoul, Korea. [7]Woo-Suk Tae and Byung-Jo Kim contributed equally. ✉email: wstae@korea.ac.kr; nukbj@korea.ac.kr

dysfunction[1]. Dissociative atrophic changes between the lateral and medial hand muscles are also observed, and cannot be fully explained by lower motor neuron lesions, as the lateral hand muscles (APB and FDI) and the medial hand muscle (ADM) are innervated by the same myotome (C8, T1 level). Additionally, the FDI and ADM are innervated by the same peripheral nerve (ulnar nerve). Therefore, it is difficult to explain solely in anatomical aspects. it can be inferred that the pathophysiology of the split-hand phenomenon is more likely associated with upper motor neuron dysfunction than with lower motor neuron dysfunction. Previous studies using electrophysiological tools have further reported that the corticomotoneuronal projections to the lateral hand muscles are more affected in ALS than those to the medial hand muscle[8,9]. These findings indicate that dysfunction of the corticomotoneuronal pathway may be the primary pathophysiology underlying the split-hand phenomenon.

Recent studies using advanced magnetic resonance imaging (MRI) techniques, particularly diffusion tensor imaging (DTI)-derived metrics of the integrity of white matter tracts, have demonstrated widespread degenerative changes in both motor and nonmotor areas of the brain in ALS. One meta-analysis study pooling 57 studies with 2,064 patients with ALS revealed the white matter degenerative changes in ALS[10]. This meta-analysis demonstrated that the most frequent alterations were observed along the corticospinal tract, followed by notable changes in the corticorubral and corticopontine tract. In addition, our previous study also revealed extensive brain white matter degenerative change in patients with ALS compared to healthy controls, affecting not only the corticospinal tract but also extra-motor regions[11]. Based on these findings, we speculate that degenerative change in the brain detected by DTI, particularly in the corticospinal tract (CST), could be associated with the split-hand phenomenon. This is further supported by experimental evidence indicating a direct link between dexterity and integrity of the CST, as shown by the selective loss of precision grip following brainstem pyramidectomy[12]. Evidence for an association between impaired CST integrity and the split-hand phenomenon is lacking, but would address an important knowledge gap in the pathophysiology of ALS, potentially offering a pathomechanistic explanation for the association between dissociative hand muscle atrophy in ALS. Therefore, the present study aimed to investigate whether the split-hand phenomenon is related to impaired integrity of the white matter tracts in the brain using DTI. To this end, in the present study, we applied tract-based spatial statistics to characterize the association between the integrity of the CST and other major brain white matter tracts and the severity of neurophysiological markers of the split-hand sign, as well as the differential pattern of the brain white matter between patients with ALS with and without the split-hand phenomenon.

Results

Clinical characteristics of study subjects

A total of 36 patients with ALS were recruited for this study. Among them, one patient with bilateral diffuse hand muscle atrophy was excluded. Finally, 35 patients (18 male; median age: 66.0 years) were enrolled (Fig. 1). A total of 35 patients with ALS (70 hands in total) were included in this study. Among them, 11 patients exhibited no split-hand phenomenon in either hand, while 24 patients showed a split-hand phenomenon in one or both hands. Among the 11 ALS patients without the split-hand phenomenon, four had atrophic changes in the ADM muscle (CMAP amplitude < 5 mV). Of these four patients, one had bilateral ADM muscle atrophy, while the other three had unilateral atrophy. Therefore, out of 70 hands, five had a reduced CMAP amplitude in the ADM muscle (< 5 mV). The median disease duration was 15.9 months, while the median ALSFRS-R score and ΔALSFRS-R were 39.0 and 0.59, respectively. Demographic and clinical data are summarized in Table 1. The lower SHI_{CMAP} between both hands was defined as the representative value of SHI_{CMAP} of each patient. The median representative value of the SHI_{CMAP} was 1.74 (IQR, 0.30–4.42).

Correlation between SHI_{CMAP} and clinical data

The representative value of the SHI_{CMAP} were negatively correlated with age at the time of the study (r=–0.390, p = 0.019), as well as the age at disease onset (r=–0.390, p = 0.022). The representative value of SHI_{CMAP} was not significantly correlated with disease duration (r=–0.059, p = 0.738), ALSFRS-R (r = 0.110, p = 0.539), or ΔALSFRS-R (r=–0.290, p = 0.100). However, the representative value of SHI_{CMAP} was positively correlation with the ALSFRS-R upper limb subscale score (r = 0.370, p = 0.033). In addition, there were no correlations between SHI_{CMAP} and the other ALSFRS-R subscale scores.

Analysis 1: correlation between electrophysiological data and DTI scalars

In the voxel-wise correlation analysis of brain white matter tracts, SHI_{CMAP} was found to be positively correlated with AD values in both the ipsilateral and contralateral sides of the posterior limb of internal capsule (PLIC), cerebral peduncle (CP), anterior limb of internal capsule (ALIC), the body of corpus callosum (BCC), external capsule, anterior corona radiata (ACR), superior corona radiata (SCR), and middle cerebellar peduncle (MCbP; $p_{FWE-corrected}$<0.05; Fig. 2). In addition, SHI_{CMAP} positively correlated with MO values in the ipsilateral and contralateral sides of the PLIC and CP and the ipsilateral superior cerebellar peduncle (SCbP; $p_{FWE-corrected}$<0.05; Fig. 2). However, there were no statistically significant differences between SHI_{CMAP} and FA, MD, and RD scalars. The CMAP amplitude of the APB was positively correlated with the AD and MO values in the ipsilateral and contralateral sides of the PLIC and the MO value in the SCbP ($p_{FWE-corrected}$<0.05; Fig. 2). The CMAP amplitude of the FDI was positively correlated with the FA, AD, and MO values on the ipsilateral and contralateral sides of the PLIC and the AD and MO values on the ipsilateral and contralateral sides of the CP ($p_{FWE-corrected}$<0.05; Fig. 2). In addition, the CMAP amplitude of the FDI was positively correlated with the AD value on the ipsilateral and contralateral sides of the MCbP, ACR, SCR, BCC, and MO values on the ipsilateral and contralateral sides of the SCbP and SCR ($p_{FWE-corrected}$<0.05; Fig. 2). The CMAP amplitude of the ADM was positively correlated with the AD value on the ipsilateral and contralateral sides of the PLIC and the ipsilateral SCR and the MO value on

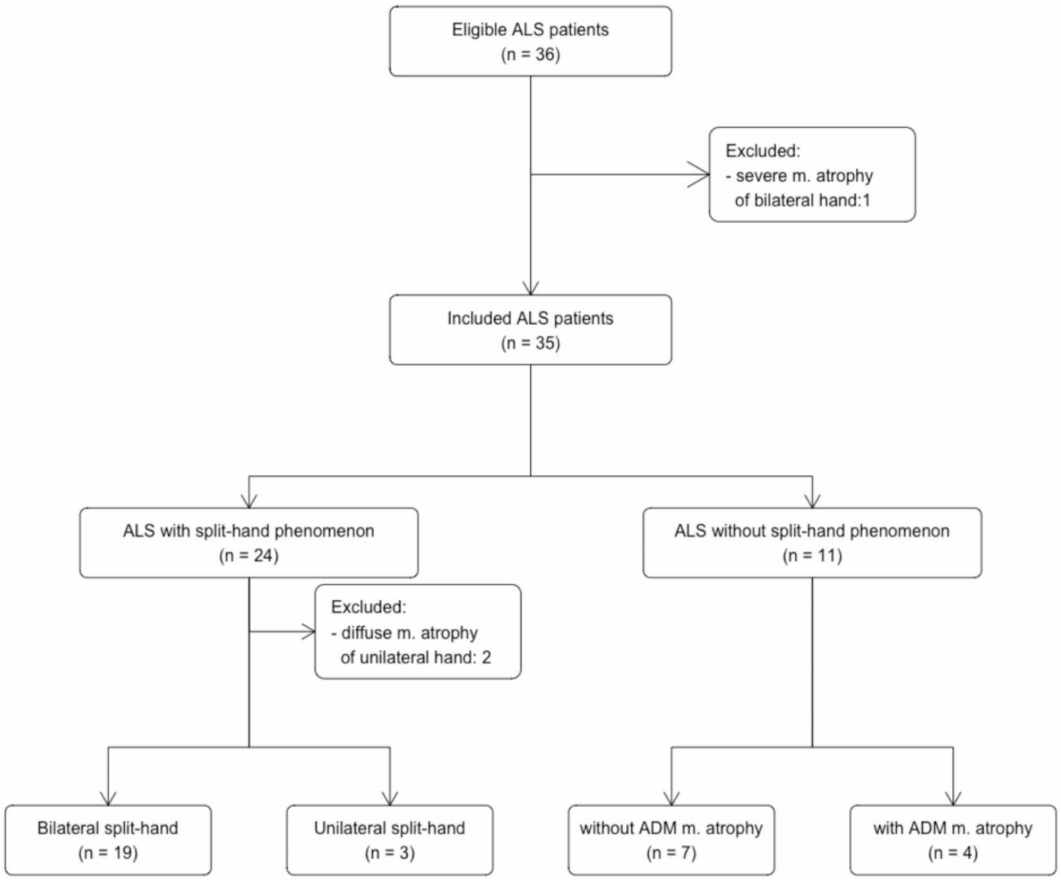

Fig. 1. Flowchart of the study population. This study enrolled 36 patients with a clinical definition of probable amyotrophic lateral sclerosis (ALS) who had undergone both MRI and a nerve conduction study on the bilateral upper limbs. One patient with diffuse hand muscle atrophy was excluded. Ultimately, 35 patients with ALS were enrolled in this study. Among these, 24 patients with ALS had the split-hand phenomenon, and 11 did not. Abbreviation: ALS, amyotrophic lateral sclerosis; NCS, nerve conduction study; ADM, abductor digiti minimi.

the contralateral side of the PLIC ($p_{FWE-corrected}<0.05$; Fig. 2). There were no statistically significant differences between the CMAP amplitudes of each hand muscle and the MD or RD scalars.

Analysis 2: group comparison of the DTI scalars between hands with and without the split-hand phenomenon

A total of 70 hands were assessed for the split-hand phenomenon, of which 43 hands tested positive, and 27 tested negative. Of the 27 hands without the split-hand phenomenon, one had predominant atrophy in the ADM, one had diffuse hand muscle atrophy, and five had reduced CMAP amplitude of the ADM (< 5 mA). The clinical and electrophysiological data are summarized in Table 2. In the voxel-wise analysis of brain white matter tracts, hands with the split-hand phenomenon showed reduced AD values on the ipsilateral and contralateral sides of the PLIC and reduced MO values on the ipsilateral and contralateral sides of the PLIC, CP, and SCbP ($p_{FWE-corrected}<0.05$; Fig. 3).

To reduce the age-effect, further analysis was performed on a sub-cohort of ALS patients aged between 50 and 80. The median age at the study time was 66.0 years in a group of hands with the split-hand phenomenon, and 62.0 years in a group of hands without the split-hand phenomenon. There was no significant age difference between two groups ($p = 0.11$). Clinical and electrophysiological data were summarized in supplementary table. In voxel-wise analysis of brain white matter tracts, a group of hands with the split-hand phenomenon showed reduced AD value in the contralateral side of the PLIC and CP ($P_{FWE-corrected}$ <0.05; supplement figure). In addition, a group of the hands with the split-hand phenomenon exhibited reduced MO value on both ipsilateral and contralateral side of PLIC, CP and SCbP ($P_{FWE-corrected}$ <0.05; supplement figure).

Analysis 3: group comparison of DTI scalars between patients having ALS with bilateral split-hand phenomenon and those with no split-hand phenomenon

A total of 24 patients with ALS experienced the split-hand phenomenon, of whom 19 had bilateral split-hand phenomenon. A further 11 patients having ALS without the split-hand phenomenon were included, of whom four had atrophic changes in the ADM. Group comparisons of DTI scalars were performed between patients

Variables	*N* = 35
Sex, male	18 (51.43%)
Age at the time of the study[a], years	66.00 (47.00–93.00)
Age at disease onset[a], years	65.00 (46.00–93.00)
Disease duration, months	15.87 (5.67–29.50)
Onset region, number	
Bulbar	11 (31.43%)
Upper limb	16 (45.71%)
Lower limb	8 (22.86%)
ALSFRS-R score[b]	39.00 (34.00–42.00)
ΔALSFRS-R[b]	0.59 (0.31–1.31)
MMSE[b]	27.00 (25.00–28.75)

Table 1. Clinical characteristics of the total study population. All categorical variables are presented as n (%); All continuous variables were presented as median (IQR), except for Age at the time of the study and Age at disease onset. ΔALSFRS-R was calculated by following formula: (48-ALSFRS-R)/disease duration. [a] Age at the time of the study and age at disease onset are presented as the median (range); [b] 34 patients with ALS were included in these variables. ALSFRS-R: revised amyotrophic lateral sclerosis functional rating scale; MMSE, mini-mental state examination.

with ALS with ($n = 19$) and without ($n = 7$) the split-hand phenomenon or hand muscle atrophy. The clinical and electrophysiological data of the two groups are summarized in Table 3. In the voxel-wise analysis of brain white matter tracts, patients having ALS with bilateral split-hand phenomenon showed reduced AD values in the left PLIC and CP and reduced MO values in the bilateral ALIC, PLIC, CP, ACR, SCR, SCbP, left MCbP, and BCC, compared to those without the split-hand phenomenon ($p_{FWE-corrected}<0.05$; Fig. 4).

Discussion

This study demonstrated that the most established electrophysiological marker of the split-hand phenomenon (SHI_{CMAP}) correlated with the loss of axonal integrity in the CST and the cerebellar and frontal association fiber tracts, as indexed by increased axial diffusivity. To disentangle the effects of SHI_{CMAP} as a composite score, we reported the association patterns of individual CMAP of each muscle using DTI metrics. All patterns overlapped with the axonal degeneration pattern, but with remarkable differences between the muscles. Axonal degeneration explaining the CMAP amplitude was largely confined to the CST for the APB, while it was most widespread for the FDI (involving CST, cerebellar pathways, nonmotor association, and transcallosal pathways) and interim for the less affected ADM. Group analysis confined to patients having ALS with bilateral split-hand phenomenon, excluding participants with diffuse muscle atrophy, confirmed reduced AD values in the left PLIC and CP as well as reduced MO values in the bilateral PLIC, CP, and SCbP, compared to those without the split-hand phenomenon. Overall, our findings provide evidence that the split-hand phenomenon in ALS is associated with axonal degenerative changes in the CST and nonmotor pathways, thereby shedding new light on the possible pathophysiology of this phenomenon.

Overall, our study showed that the severity of asymmetric neuromuscular function in patients with ALS was directly correlated with axonal degeneration in the CST and CP, with confirmatory support from a controlled subgroup comparison showing that patients having ALS with the split-hand phenomenon had reduced AD and MO values in the PLIC and CP compared to those without the split-hand phenomenon. DTI measures the movement of water molecule in tissue and assesses microstructural changes in the brain. Among DTI scalars, FA, the most commonly used DTI scalar, reflects diffusional asymmetry. AD measures diffusivity along the principal axis of the neural tract, linked to axonal damage, while RD represents mean diffusivity along the minor axes, indicating myelin damage. MD averages the three orthogonal diffusivities, reflecting tissue size and integrity. MO describes the type of anisotropy, showing diffusion tensor shape variations from planar to linear. Our findings suggest that the split-hand index is more closely related to AD and MO scalars than to FA, RD, and MD scalars. This may indicate that the split-hand phenomenon is primarily associated with axonal degeneration and linear diffusion tensor changes rather than with demyelination and planar diffusion tensor alterations.

Our findings could support the hypothesis that corticomotor dysfunction is associated with the pathogenesis of the split-hand phenomenon in ALS. Although the exact pathogenesis of the split-hand phenomenon remains unclear, corticomotor dysfunction is considered the primary cause of this condition. Previous studies have suggested that the corticomotoneuronal input to the lateral hand muscle complex is preferentially defective in ALS, compared to the medial hand muscles[8]. In addition, previous studies have demonstrated that, compared to normal controls, ALS patients exhibited reduced short-interval intracortical inhibition, an electrophysiological biomarker of cortical excitability, in intrinsic hand muscles, with a notably more pronounced decrease in the APB/FDI muscles[9,13]. These findings imply that cortical hyperexcitability is significantly more prominent in the lateral hand muscle complex than in the medial hand muscles. This dissociative pattern of cortical hyperexcitability may be associated with the pathogenesis of the split-hand phenomenon. Furthermore, the split phenomenon in ALS has been observed not only in the hand, but also in different body parts, including the elbow (the split-elbow)[14,15], leg (the split-leg)[16,17], and foot (the split-foot)[18,19]. Ludolph et al. previously reported that patients

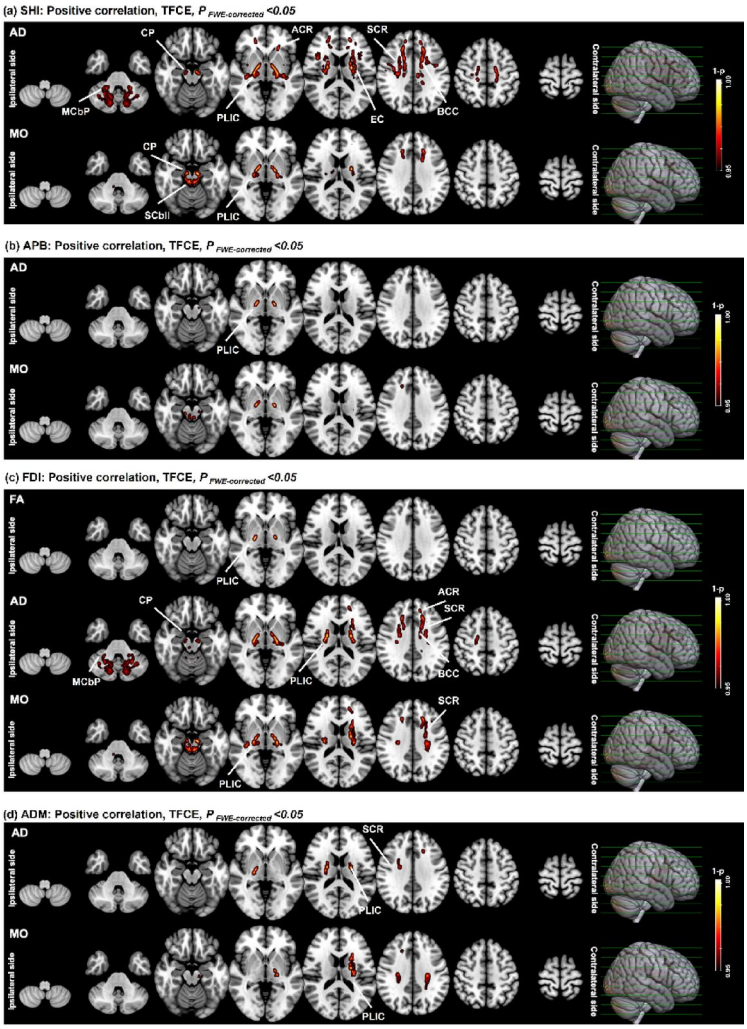

Fig. 2. Tract-based spatial statics analysis: A correlation analysis between diffusion tensor imaging scalars and electrophysiological data. Correlation analysis adjusted for age, sex, and disease duration between electrophysiological data and diffusion tensor imaging (DTI) scalars was performed using tract-based spatial statistics analysis. (**A**) The split-hand index (SHI) was positively correlated with the AD value on the ipsilateral and contralateral sides of the posterior limb of the internal capsule (PLIC), cerebral peduncle (CP), anterior corona radiata (ACR), superior corona radiata (SCR), external capsule (EC), body of the corpus callosum (BCC), and middle cerebellar peduncle ($p_{FWE-corrected}$<0.05). In addition, SHI positively correlated with MO values on both the ipsilateral and contralateral sides of the PLIC, CP, and superior cerebellar peduncle (SCbP). (**B**) The compound muscle action potential (CMAP) amplitude of the abductor pollicis brevis (APB) was positively correlated with AD and MO values on the ipsilateral and contralateral sides of the PLIC ($p_{FWE-corrected}$<0.05). (**C**) The CMAP amplitude of the first dorsal interosseous (FDI) muscle was positively correlated with the FA value in the ipsilateral and lateral sides of the PLIC ($p_{FWE-corrected}$<0.05); the AD value in the ipsilateral and contralateral sides of the PLIC, MCbP, ACR, SCR, and BCC ($p_{FWE-corrected}$<0.05); and the MO value in the ipsilateral and contralateral sides of the PLIC, SCbP, and SCR ($p_{FWE-corrected}$<0.05). (**D**) The CMAP amplitude of the abductor digiti minimi (ADM) was positively correlated with the AD value in the ipsi- and contra-lateral side of the PLIC and ipsilateral SCR ($p_{FWE-corrected}$<0.05), and MO value in the contra-lateral side of PLIC ($p_{FWE-corrected}$<0.05). Abbreviations: FA, fraction anisotropy; AD, Axial diffusivity; MO, mode of anisotropy; TFCE, Threshold-Free Cluster Enhancement; FWE, the familywise error; SHI, split-hand index; APB, abductor pollicis brevis; FDI, first dorsal interosseous; ADM, abductor digiti minimi; PLIC, posterior limb of internal capsule; CP, cerebral peduncle, ACR, anterior corona radiata; SCR, superior corona radiata; MCbP, middle cerebellar peduncle; EC, external capsule; BCC, body of corpus callosum.

with ALS exhibit greater relative weakness in the thumb abductor, hand extensor, elbow flexor, knee flexor, and plantar extensor muscles[20]. These muscle groups may be more prominently affected in ALS owing to their strong corticomotoneuronal connectivity. These findings indicate that the degeneration of the corticomotoneuronal system could be a major contributing factor to the pathogenesis of the split-hand phenomenon in ALS.

The split-hand phenomenon is considered an early and distinct feature of ALS. However, it has also been reported in other diseases, including spinal and bulbar muscular atrophy (SBMA) and GARS1-associated

Variable	Hands without the split-hand phenomenon	Hands with the split-hand phenomenon	*p*-value[2]
Number	20	43	
Sex, male	9.0 (45.0%)	23.0 (53.5%)	0.5
Age at the time of the study [a], years	58.50 (47.00, 77.00)	68.00 (51.00, 93.00)	0.003
Age at disease onset [a], years	55.50 (46.00, 76.00)	67.00 (51.00, 93.00)	0.003
Disease duration, months	18.60 (2.90, 41.93)	12.57 (0.80, 60.90)	0.3
Onset region			< 0.001
Bulbar	5.0 (25.0%)	14.0 (32.6%)	
Upper limb	3.0 (15.0%)	26.0 (60.5%)	
Lower limb	12.0 (60.0%)	3.0 (7.0%)	
CMAP amplitude			
APB muscle	8.05 (3.80, 12.20)	2.20 (0.00, 9.10)	< 0.001
FDI muscle	10.30 (4.80, 15.00)	3.60 (0.00, 17.90)	< 0.001
ADM muscle	10.00 (5.90, 11.70)	6.80 (1.50, 17.10)	0.002
Split-hand index	9.04 (3.09, 13.16)	1.50 (0.00, 8.27)	< 0.001

Table 2. Comparison of clinical and electrophysiological data between hands with and without the split-hand phenomenon. All categorical variables were presented as n (%); All continuous variables were presented as median (IQR), except for Age at the time of the study and Age at disease onset. [a] Age at the time of the study and age at disease onset are presented as the median (range). Abbreviation: CMAP, compound muscle action potential; APB, abductor pollicis brevis; FDI, first dorsal interosseous; ADM, abductor digiti minimi; SHI, split-hand index.

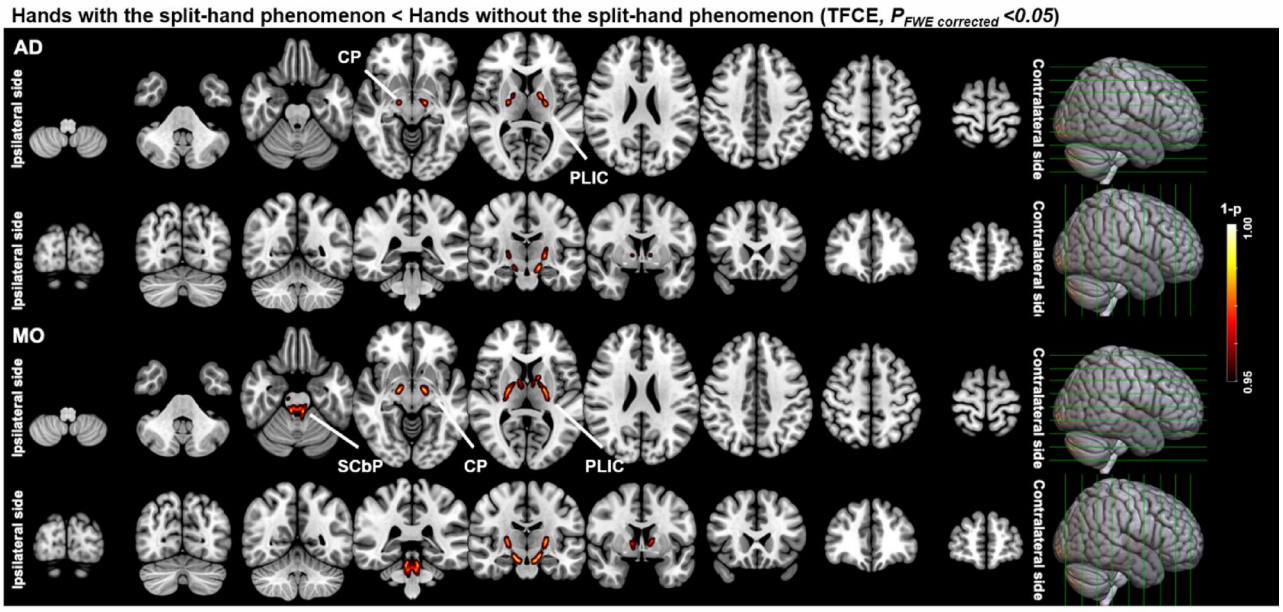

Fig. 3. Tract-based spatial statics analysis: A group comparison of diffusion tensor imaging scalars between hands with and without the split-hand phenomenon. Group comparisons adjusted for age, sex, and disease duration between hands with and without the split-hand phenomenon were performed using tract-based spatial statistical analysis. Hands with the split-hand phenomenon showed reduced axial diffusivity on the contralateral side of the posterior limb of the internal capsule (PLIC) and cerebral peduncle (CP) compared with hands without the split-hand phenomenon ($p_{FWE-corrected}$<0.05). Hands with the split-hand phenomenon had a reduced mode of anisotropy value in the ipsilateral and contralateral sides of the PLIC, CP, and superior cerebellar peduncle compared to the hands without the split-hand phenomenon ($p_{FWE-corrected}$<0.05). TFCE, Threshold-Free Cluster Enhancement; FWE, familywise error; AD, axial diffusivity; MO, mode of anisotropy; CP, cerebral peduncle; PLIC, posterior limb of internal capsule; SCbP, superior cerebellar peduncle.

Variable	ALS with bilateral split-hand phenomenon	ALS without split-hand phenomenon	*p*-value
Number	19	7	
Sex, male	10 (52.6%)	3 (42.9%)	> 0.9
Age at the time of the study, years	72.25 (62.30, 78.88)	57.86 (56.72, 64.81)	0.073
Age at disease onset, years	67.73 (61.48, 74.68)	54.42 (54.42, 63.53)	0.049
Disease duration, months	12.57 (3.77, 32.48)	18.60 (13.67, 28.00)	0.5
Onset region, number			< 0.001
Bulbar	6 (31.6%)	0 (0.0%)	
Upper limb	12 (63.2%)	1 (14.3%)	
Lower limb	1 (5.3%)	6 (85.7%)	
ALSFRS-R score[a]	39.00 (37.00, 42.00)	39.00 (31.50, 41.50)	0.7
ΔALSFRS-R[a]	0.89 (0.24, 1.65)	0.58 (0.43, 0.61)	0.6
CMAP amplitude, right			
APB muscle	1.90 (0.30, 4.80)	7.60 (7.10, 8.80)	< 0.001
FDI muscle	3.00 (1.95, 7.35)	13.00 (11.10, 13.70)	< 0.001
ADM muscle	5.70 (4.20, 9.65)	11.00 (10.70, 11.50)	0.032
CMAP amplitude, left			
APB muscle	2.20 (1.00, 3.05)	9.40 (7.80, 9.60)	< 0.001
FDI muscle	3.50 (1.60, 5.60)	9.80 (9.45, 12.45)	0.005
ADM muscle	5.60 (4.45, 8.15)	9.80 (8.45, 10.40)	0.022
Right SHI_{CMAP}	1.01 (0.12, 2.30)	9.08 (8.51, 10.06)	< 0.001
Left SHI_{CMAP}	1.19 (0.30, 2.03)	9.44 (8.76, 10.73)	< 0.001
Representative SHI_{CMAP}	0.50 (0.06, 1.49)	8.51 (8.03, 9.05)	< 0.001

Table 3. Comparison of clinical and electrophysiological data between ALS with and without split-hand phenomenon. All categorical variables were presented as n (%); All continuous variables were presented as median (IQR). [a]18 ALS patients with bilateral split-hand phenomenon were included in these variable. Abbreviation: ALSFRS-R: revised amyotrophic lateral sclerosis functional rating scale; MMSE, mini-mental state examination; CMAP, compound muscle action potential; APB, abductor pollicis brevis; FDI, first dorsal interosseous; ADM, abductor digiti minimi; SHI, split-hand index.

neuropathy[21,22]. SBMA and GARS1-associated neuropathy are traditionally thought to involve only lower motor neurons. These findings suggest that the pathomechanism of the split-hand phenomenon is more complex, potentially involving not only cortical dysfunction but also other mechanisms, such as spinal motoneuron dysfunction, peripheral nerve excitability, and neuromuscular junction dysfunction. Shibuya et al. reported that nerve excitability was more pronounced in patients with SBMA who exhibited the split-hand phenomenon compared to those without it, whereas this pattern was not observed in ALS[21]. In SBMA, the split-hand phenomenon may be related to increased nerve excitability. However, in ALS, the involvement of upper motor neuron dysfunction cannot be ruled out. Interestingly, a recent study reported that central nervous system (CNS) neurodegeneration was observed in SBMA[23], indicating that motor cortical hyperexcitability may also contribute to the split-hand phenomenon in SBMA. Further studies are needed to clarify these mechanisms.

Our study revealed that the CMAP amplitude of each hand muscle positively correlated with the AD and MO values of the CST in patients with ALS. The CMAP amplitude further represents the summed action potentials of all depolarized muscle fibers. Reduced CMAP amplitudes can be caused by neuropathy, neuromuscular junction disorders, or myopathy. In ALS, the reduced CMAP amplitude is primarily attributable to neuropathy, particularly the loss of axons, as ALS is a motor neuron disease that affects both upper and lower motor neurons. Among several DTI scalars, the AD scalar is considered a reliable indicator of axonal dysfunction[24]. Therefore, our findings indicate that axonal degeneration of the CST in the brain may be linked to peripheral nerve axonal dysfunction. Additionally, one prior study using transcranial magnetic stimulation (TMS) reported that the FA value of the CST was correlated with TMS parameters[25]. However, further research utilizing multimodal neuroimaging and electrophysiological methods, such as a combination of DTI, TMS, and NCS, may better elucidate this issue.

Interestingly, our study indicated that the $SHI_{CMAP}$is associated with the cerebellar peduncle and corpus callosum. The cerebellum plays an essential role, not only in coordinating movement and balance, but also in controlling finger movement. Previous studies have similarly reported impaired precision grip in patients with cerebellar lesions[26,27]. These results suggest that the cerebellum plays a crucial role in precision grip. In addition, the corpus callosum may be involved in motor functions. The corpus callosum is an important structure that connects the two brain hemispheres, while the motor corpus callosum connects the primary motor cortex between the two hemispheres. One previous study reported that the hand callosal motor fibers were positively correlated with the hand area of the primary motor cortex[28]. This indicates that the corpus callosal degeneration could contribute to motor dysfunction. In summary, our findings indicate that the split-hand phenomenon may be associated with not only the motor pathway, but also the nonmotor pathway in ALS.

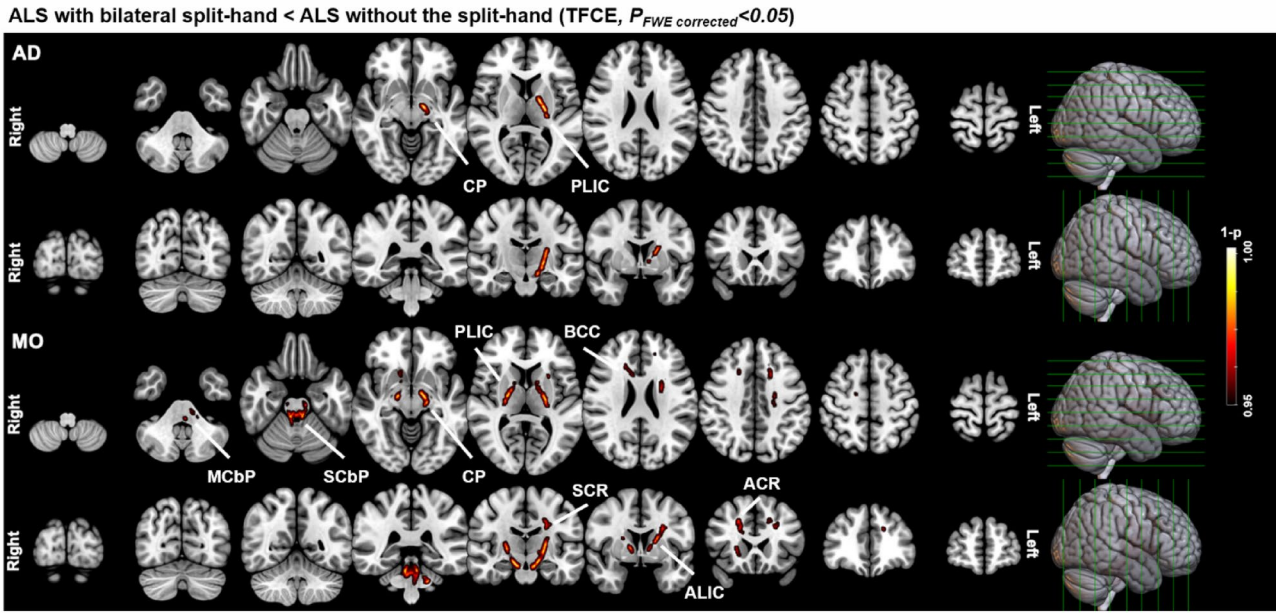

Fig. 4. Tract-based spatial statics analysis: A group comparison of diffusion tensor imaging scalars between patients having amyotrophic lateral sclerosis with and without the split-hand phenomenon. Group comparisons adjusted for age, sex, and disease duration between patients with amyotrophic lateral sclerosis (ALS) with and without the split-hand phenomenon were performed using tract-based spatial statistical analysis. Patients having ALS with bilateral split-hand phenomenon showed reduced axial diffusivity in the left posterior limb of the internal capsule (PLIC) and cerebral peduncle (CP) compared with those without the split-hand phenomenon ($p_{FWE-corrected}$<0.05). ALS with bilateral split-hand phenomenon reduced the mode of anisotropy value in the bilateral PLIC, CP, anterior limb of the internal capsule, anterior and superior corona radiata, superior cerebellar peduncle, left middle cerebellar peduncle, and body of the corpus callosum ($p_{FWE-corrected}$<0.05). Abbreviation: ALS, amyotrophic lateral sclerosis; TFCE, Threshold-Free Cluster Enhancement; FWE, the familywise error; AD, axial diffusivity; MO, the mode of anisotropy; CP, cerebral peduncle; PLIC, posterior limb of internal capsule; MCbP, middle cerebellar peduncle; SCbP, superior cerebellar peduncle; BCC, body of corpus callosum; SCR, superior corona radiata; ACR, anterior corona radiata; ALIC, anterior limb of internal capsule.

Although its role in the pathogenesis of ALS remains controversial, several studies have indicated that cortical hyperexcitability could be the main pathogenetic process underlying ALS[29,30]. Previous studies have further demonstrated that patients with ALS exhibit cortical hyperexcitability in both the dominant and nondominant primary motor cortex, with a more pronounced effect over the dominant motor cortex[31]. Furthermore, cortical hyperexcitability can precede lower motor neuron dysfunction in ALS[32]. A recent study using optical coherence tomography revealed that the retinal nerve fiber layer thickness, which may be associated with neurodegeneration in the CNS, was thinner in ALS compared to healthy controls, suggesting it could be a potential biomarker of disease progression in ALS[33]. In addition, impairment of proteostasis and ribostasis in the CNS is considered one of the common pathomechanisms in age-related neurodegenerative disease, including ALS[34]. Taken together, our findings support the "dying forward" hypothesis, which proposes that motor neuron degeneration is mediated by corticomotoneuronal dysfunction, and progresses through anterograde degeneration of the distal axons. This hypothesis may explain the pathogenesis of ALS.

In our study, SHI_{CMAP} was negatively correlated with age at the time of the study and at onset. Previous studies have reported that CMAP amplitudes of the APB, FDI, and ADM, as well as SHI_{CMAP}were negatively correlated with age[35,36], and that the APB and FDI were more affected by age than the ADM[35]. These findings suggest that aging could influence degenerative changes in peripheral nerves, neuromuscular junctions, or muscles, thereby augmenting the pathomechanism underlying the split-hand phenomenon. However, the factors that determine the differences in age effects between the medial and lateral hand muscles remain unknown. Corticomotoneuronal fiber degeneration associated with aging may be a contributing factor. As such, further studies are required to confirm this hypothesis. In addition, these findings suggest that the effect of age on SHI_{CMAP} should be considered when diagnosing ALS or planning research using SHI_{CMAP}.

Our study has some limitations. First, the study population, particularly the subgroup of subjects with unilateral or no split-hand phenomenon, was very small. However, a comparison between ipsilateral and contralateral symptoms in patients with ALS with unilateral split-hand phenomenon could be helpful in elucidating its pathogenesis. As such, further studies with larger sample sizes are required to clarify this issue. Second, the MRI acquisition parameters in this study included a slice thickness of 3 mm. This thickness may have resulted in to partial volume effects, potentially reducing the sensitivity of DTI to demyelination. Consequently, our study may have underestimated demyelination-related changes, and this limitation should be considered when interpreting

the results. Further studies using thinner slice thicknesses will be necessary to clarify this issue. Third, our study handled the missing data using the pairwise deletion methods, which has some limitations such as potential bias, reduced comparability, and loss of statistical power. Our DTI and electrophysiological data had no missing values, whereas some clinical variables, including ALSFRS-R, delta ALSFRS-R, and MMSE scores, had missing data. So, our findings need to be interpreted with these considerations in mind. Fourth, this study was unable to determine the sample size through power analysis. To the best of our knowledge, no studies have investigated the split-hand phenomenon and brain microstructural changes using DTI data. Given the limited research on this topic and the absence of effect size estimates, a power analysis for sample size determination was not feasible. Future studies with an optimal sample size are needed to enhance the validity of these findings. Fifth, this study lacked a normal control group. Future studies with normal controls are needed to contextualize our findings with normative DTI data and better understand the implications of our results.

In conclusion, our study demonstrated that the split-hand phenomenon may be linked to degenerative changes in the corticomotor pathway. Our findings indicate that dysfunction in the corticomotoneuronal connections may be the primary cause of this phenomenon. Additionally, our results imply that such dysfunction could be a critical factor in the development of ALS, highlighting a possible area of focus for understanding its pathogenesis and developing therapeutic targets.

Methods

Study population and clinical data

Patients with clinically probable or definite ALS according to the revised El Escorial criteria[37] were prospectively recruited from the neurology clinic of a university-affiliated hospital between January 2017 and December 2022. All patients underwent both a brain MRI scan and a nerve conduction study (NCS) of bilateral median and ulnar nerves, with recording from the APB, FDI, and ADM muscles. Patients with ALS for whom the split-hand index could not be computed due to non-evoked CMAPs in hand muscles, resulting from severe hand muscle atrophy were excluded. The collected demographic and clinical data included age at disease onset, age at the time of the study, sex, disease duration at the time of the study, onset region, ALS functional rating scale-revised (ALSFRS-R) score, and ΔALSFRS-R at the time of the DTI study. The ΔALSFRS-R was calculated using the following equation: (48 – ALSFRS-R score at the time of DTI study)/disease duration at the time of DTI study (months). The ALSFRS-R scores were divided into four subscales: bulbar, upper limb, lower limb, and respiratory.

This study was approved by the Institutional Review Board (IRB) of Korea University Anam Hospital (IRB number: 2015 AN0337), and was performed in accordance with the principles of the Declaration of Helsinki and all relevant institutional guidelines and regulations. Written informed consent was obtained from all participants prior to inclusion.

Electrophysiological data

NCS was performed using standard electrodiagnostic equipment (Viking and Synergy; Nicolet EDX system; Natus Medical, Middleton, WI, USA). The median nerve was stimulated at the wrist and recorded at the APB. The ulnar nerve was stimulated at the wrist and recorded at the FDI and ADM. Each nerve was further stimulated with supramaximal stimulus intensity. The recording electrode was a 1-cm-diameter, disposable, flat-surface electrode placed on the belly of each muscle. The SHI was calculated using the CMAP amplitude of each muscle according to the following equation: $SHI_{CMAP} = (APB_{CMAP} \times FDI_{CMAP})/ADM_{CMAP}$.

MRI acquisition and image processing

Brain MRI data were acquired using a 3 T Prisma MRI scanner (Siemens Healthineers, Erlangen, Germany). Diffusion-weighted MRI was further performed with an echo-planar imaging sequence with the following parameters: a B0 image serves as a reference for subsequent 64 gradient diffusion-weighted directional images with a b-value of 1000 s/mm^2, and additional 31 B0 images for better signal averaging, which improves the signal-to-noise ratio and helps with EPI distortion correction for motion and eddy current effects. A repetition time of 3900 ms, an echo time of 55 ms, a field of view of 224 × 224 mm, a matrix size of 112 × 112, and a slice thickness of 3.0 mm.

MRI data were pre-processed using the Nottingham NIHR Biomedical Research Centre pipeline (version 1.6.5)[38]. Preprocessing included skull stripping, eddy current correction, echo planar imaging distortion correction, motion correction, linear/nonlinear registration to anatomical/standard space, generation of microstructure maps, and quality control checks.

Tract-Based Spatial statistics analysis preprocessing

Using the Tract-Based Spatial Statistics (TBSS) tool of the Functional MRI of the Brain (FMRIB) Software Library Software Library (FSL version 6.0.7.3; Oxford, U.K.; http://www.fmrib.ox.ac.uk/fsl/)[39], the fraction anisotropy (FA) images of each participant were aligned to the FMRIB58_FA_template image and transformed into a 1 × 1 × 1 mm^3 standard space (Montreal Neurological Institute 152 standard) using the FMRIB Nonlinear Image Registration Tool. Resulting transformation matrices were subsequently applied to the original FA images for each participant. An averaged FA image was generated using the transformed FA images, and extracted to create a mean FA skeleton image representing the centers of all the white matte tracts. The FA skeleton image was then set to a threshold of FA > 0.2 to include the major white matter pathways. Each mean diffusivity (MD), mode of anisotropy (MO), axial diffusivity (AD), and radial diffusivity (RD) skeleton image was extracted using the FSL command line tool "*tbss_non_FA*." Quality control (QC) was performed using FSL Eddy QC tool "*eddy_quad*."

Subgroup and statistical analyses

For clinical data, the Wilcoxon rank-sum test was applied to compare continuous variables, while the chi-squared test was used to compare categorical variables. Correlation analysis was performed using Pearson's correlation analysis between the SHI_{CMAP} and the clinical data. Statistical analyses were performed using R (version 4.4.0; R Foundation for Statistical Computing). Statistical significance was set at $p < 0.05$.

All five DTI scalars (FA, MD, MO, AD, and RD) were used for the DTI data. Subgroups were defined based on the presence of the split-hand phenomenon, defined as a ratio of FDI/ADM CMAP amplitude ratio or a APB/ADM CMAP amplitude ratio of < 0.6[40]. Three primary analyses were performed with five scalars each: (1) correlation analysis with covariates (age, sex, and disease duration) was performed between each DTI scalar and electrophysiological data (SHI_{CMAP} and CMAP amplitude of each muscle); (2) asymmetries of tract-based DTI metrics between the most and least affected hemispheres were compared between the ipsilateral and contralateral hemispheres of the hands, with and without the split-hand phenomenon; and (3) ALS cases with bilateral split-hand phenomenon were compared with those without the split-hand phenomenon.

Although motor function generally originates from the contralateral motor cortex, some studies have reported that the ipsilateral motor cortex may also contribute to limb control[41]. To consider this factor, we analyzed the correlation between electrophysiologic data from each side and DTI values in both contralateral and ipsilateral hemispheres using a method previously applied in DTI study of patients with ALS[42]. For these analyses, the electrophysiological data from the right hand were compared with each participant's 'unflipped' DTI image, while the electrophysiological data from the left hand were compared with each participant's 'flipped' DTI image. In Analysis 1 and 2, FSL's command line tool "*fslswapdim*" was used to analyze the DTI data of ipsilateral and contralateral hemispheres based on the hand during TBSS preprocessing step. FSL's command line tool "*randomise*" was applied for univariate permutations at each voxel. Group differences in FA, MD, MO, AD, and RD were examined using analysis of covariance with 5,000 permutations and age, sex, and disease duration as covariates. These results were corrected for multiple comparisons at the cluster level using Threshold-Free Cluster Enhancement[43], with the family-wise error (FWE) rate set at 5% to control for false positives. An FWE-corrected p-value of < 0.05 was considered statistically significant.

Data availability

The datasets generated during and/or analyzed during the current study are available from the corresponding author on reasonable request.

Received: 3 December 2024; Accepted: 7 April 2025
Published online: 11 April 2025

References

1. Corcia, P. et al. Split-hand and split-limb phenomena in amyotrophic lateral sclerosis: pathophysiology, electrophysiology and clinical manifestations. *J. Neurol. Neurosurg. Psychiatry*. **92**, 1126–1130. https://doi.org/10.1136/jnnp-2021-326266 (2021).
2. Simon, N. G., Lomen-Hoerth, C. & Kiernan, M. C. Patterns of clinical and electrodiagnostic abnormalities in early amyotrophic lateral sclerosis. *Muscle Nerve*. **50**, 894–899. https://doi.org/10.1002/mus.24244 (2014).
3. Menon, P., Kiernan, M. C., Yiannikas, C., Stroud, J. & Vucic, S. Split-hand index for the diagnosis of amyotrophic lateral sclerosis. *Clin. Neurophysiol.* **124**, 410–416. https://doi.org/10.1016/j.clinph.2012.07.025 (2013).
4. Pavey, N. et al. Utility of split hand index with different motor unit number Estimation techniques in ALS. *Clin. Neurophysiol.* **156**, 175–182. https://doi.org/10.1016/j.clinph.2023.09.018 (2023).
5. Kim, D. G. et al. Split-hand phenomenon in amyotrophic lateral sclerosis: A motor unit number index study. *Muscle Nerve*. **53**, 885–888. https://doi.org/10.1002/mus.24958 (2016).
6. Seok, H. Y. et al. Split hand muscle echo intensity index as a reliable imaging marker for differential diagnosis of amyotrophic lateral sclerosis. *J. Neurol. Neurosurg. Psychiatry*. **89**, 943–948. https://doi.org/10.1136/jnnp-2017-317917 (2018).
7. Lu, W. Z. et al. Split-hand index for amyotrophic lateral sclerosis diagnosis: A frequentist and bayesian meta-analysis. *Clin. Neurophysiol.* **143**, 56–66. https://doi.org/10.1016/j.clinph.2022.08.020 (2022).
8. Weber, M., Eisen, A., Stewart, H. & Hirota, N. The split hand in ALS has a cortical basis. *J. Neurol. Sci.* **180**, 66–70. https://doi.org/10.1016/s0022-510x(00)00430-5 (2000).
9. Menon, P., Kiernan, M. C. & Vucic, S. Cortical dysfunction underlies the development of the split-hand in amyotrophic lateral sclerosis. *PLoS One*. **9**, e87124. https://doi.org/10.1371/journal.pone.0087124 (2014).
10. Gorges, M. et al. Corticoefferent pathology distribution in amyotrophic lateral sclerosis: in vivo evidence from a meta-analysis of diffusion tensor imaging data. *Sci. Rep.* **8**, 15389. https://doi.org/10.1038/s41598-018-33830-z (2018).
11. Baek, S. H. et al. Usefulness of diffusion tensor imaging findings as biomarkers for amyotrophic lateral sclerosis. *Sci. Rep.* **10**, 5199. https://doi.org/10.1038/s41598-020-62049-0 (2020).
12. Lawrence, D. G. & Kuypers, H. G. The functional organization of the motor system in the monkey. I. The effects of bilateral pyramidal lesions. *Brain* **91**, 1–14. https://doi.org/10.1093/brain/91.1.1 (1968).
13. Bae, J. S., Menon, P., Mioshi, E., Kiernan, M. C. & Vucic, S. Cortical hyperexcitability and the split-hand plus phenomenon: pathophysiological insights in ALS. *Amyotroph. Lateral Scler. Frontotemporal Degener*. **15**, 250–256. https://doi.org/10.3109/21678421.2013.872150 (2014).
14. Khalaf, R. et al. Relative preservation of triceps over biceps strength in upper limb-onset ALS: the 'split elbow'. *J. Neurol. Neurosurg. Psychiatry*. **90**, 730–733. https://doi.org/10.1136/jnnp-2018-319894 (2019).
15. Pavey, N., Higashihara, M., van den Bos, M. A. J., Menon, P. & Vucic, S. The split-elbow index: A biomarker of the split elbow sign in ALS. *Clin. Neurophysiol. Pract.* **7**, 16–20. https://doi.org/10.1016/j.cnp.2021.11.002 (2022).
16. Simon, N. G. et al. Dissociated lower limb muscle involvement in amyotrophic lateral sclerosis. *J. Neurol.* **262**, 1424–1432. https://doi.org/10.1007/s00415-015-7721-8 (2015).
17. Hu, F. et al. Dissociated lower limb muscle involvement in amyotrophic lateral sclerosis and its differential diagnosis value. *Sci. Rep.* **9**, 17786. https://doi.org/10.1038/s41598-019-54372-y (2019).
18. Wang, Z. L. et al. Reassessment of Split-Leg signs in amyotrophic lateral sclerosis: differential involvement of the extensor digitorum brevis and abductor hallucis muscles. *Front. Neurol.* **10**, 565. https://doi.org/10.3389/fneur.2019.00565 (2019).
19. Min, Y. G. et al. Dissociated leg muscle atrophy in amyotrophic lateral sclerosis/motor neuron disease: the 'split-leg' sign. *Sci. Rep.* **10**, 15661. https://doi.org/10.1038/s41598-020-72887-7 (2020).

20. Ludolph, A. C. et al. Pattern of paresis in ALS is consistent with the physiology of the corticomotoneuronal projections to different muscle groups. *J. Neurol. Neurosurg. Psychiatry*. **91**, 991–998. https://doi.org/10.1136/jnnp-2020-323331 (2020).
21. Shibuya, K. et al. Split hand and motor axonal hyperexcitability in spinal and bulbar muscular atrophy. *J. Neurol. Neurosurg. Psychiatry*. **91**, 1189–1194. https://doi.org/10.1136/jnnp-2020-324026 (2020).
22. Jiménez-Jiménez, J. et al. Insights into phenotypic variability caused by GARS1 pathogenic variants. *Eur. J. Neurol.* **31**, e16416. https://doi.org/10.1111/ene.16416 (2024).
23. Tu, S. et al. Central neurodegeneration in Kennedy's disease accompanies peripheral motor dysfunction. *Sci. Rep.* **14**, 18331. https://doi.org/10.1038/s41598-024-69393-5 (2024).
24. Winklewski, P. J. et al. Understanding the physiopathology behind axial and radial diffusivity Changes-What do we know?? *Front. Neurol.* **9**, 92. https://doi.org/10.3389/fneur.2018.00092 (2018).
25. Wittstock, M., Wilde, N., Grossmann, A., Kasper, E. & Teipel, S. Mirror movements in amyotrophic lateral sclerosis: A combined study using diffusion tensor imaging and transcranial magnetic stimulation. *Front. Neurol.* **11**, 164. https://doi.org/10.3389/fneur.2020.00164 (2020).
26. Fellows, S. J., Ernst, J., Schwarz, M., Topper, R. & Noth, J. Precision grip deficits in cerebellar disorders in man. *Clin. Neurophysiol.* **112**, 1793–1802. https://doi.org/10.1016/s1388-2457(01)00623-x (2001).
27. Muller, F. & Dichgans, J. Impairments of precision grip in two patients with acute unilateral cerebellar lesions: a simple parametric test for clinical use. *Neuropsychologia* **32**, 265–269. https://doi.org/10.1016/0028-3932(94)90012-4 (1994).
28. Wahl, M. et al. Human motor corpus callosum: topography, somatotopy, and link between microstructure and function. *J. Neurosci.* **27**, 12132–12138. https://doi.org/10.1523/JNEUROSCI.2320-07.2007 (2007).
29. Vucic, S. & Kiernan, M. C. Novel threshold tracking techniques suggest that cortical hyperexcitability is an early feature of motor neuron disease. *Brain* **129**, 2436–2446. https://doi.org/10.1093/brain/awl172 (2006).
30. Van den Bos, M. A. J. et al. Imbalance of cortical facilitatory and inhibitory circuits underlies hyperexcitability in ALS. *Neurology* **91**, e1669–e1676. https://doi.org/10.1212/wnl.0000000000006438 (2018).
31. Menon, P. et al. Cortical hyperexcitability and disease spread in amyotrophic lateral sclerosis. *Eur. J. Neurol.* **24**, 816–824. https://doi.org/10.1111/ene.13295 (2017).
32. Menon, P., Kiernan, M. C. & Vucic, S. Cortical hyperexcitability precedes lower motor neuron dysfunction in ALS. *Clin. Neurophysiol.* **126**, 803–809. https://doi.org/10.1016/j.clinph.2014.04.023 (2015).
33. Taufik, S. A. et al. Longitudinal changes in the retinal nerve fiber layer thickness in amyotrophic lateral sclerosis and Parkinson's disease. *J. Clin. Neurol.* **20**, 285–292. https://doi.org/10.3988/jcn.2023.0353 (2024).
34. Lim, S. M., Nahm, M. & Kim, S. H. Proteostasis and ribostasis impairment as common cell death mechanisms in neurodegenerative diseases. *J. Clin. Neurol.* **19**, 101–114. https://doi.org/10.3988/jcn.2022.0379 (2023).
35. Pechirra, G., Swash, M. & de Carvalho, M. The senile hand: age effects on intrinsic hand muscle CMAP amplitudes influence split-hand index calculations. *Muscle Nerve*. **65**, 463–467. https://doi.org/10.1002/mus.27489 (2022).
36. Zoccolella, S. et al. Neurophysiological indices for split phenomena: correlation with age and sex and potential implications in amyotrophic lateral sclerosis. *Front. Neurol.* **15**, 1371953. https://doi.org/10.3389/fneur.2024.1371953 (2024).
37. Brooks, B. R., Miller, R. G., Swash, M. & Munsat, T. L. El Escorial revisited: revised criteria for the diagnosis of amyotrophic lateral sclerosis. *Amyotroph. Lateral Scler. Other Motor Neuron Disord*. **1**, 293–299. https://doi.org/10.1080/146608200300079536 (2000).
38. Mohammadi-Nejad, A. R., Pszczolkowski, S., Auer, D. & Sotiropoulos, S. Multi-modal neuroimaging pipelines for data preprocessing. Zenodo, (2023).
39. Jenkinson, M., Beckmann, C. F., Behrens, T. E., Woolrich, M. W. & Smith, S. M. *FSL Neuroimage* **62**, 782–790, https://doi.org/10.1016/j.neuroimage.2011.09.015 (2012).
40. Kuwabara, S. et al. Dissociated small hand muscle atrophy in amyotrophic lateral sclerosis: frequency, extent, and specificity. *Muscle Nerve*. **37**, 426–430. https://doi.org/10.1002/mus.20949 (2008).
41. Ding, H. et al. The role of ipsilateral motor network in upper limb movement. *Front. Physiol.* **14**, 1199338. https://doi.org/10.3389/fphys.2023.1199338 (2023).
42. Douaud, G., Filippini, N., Knight, S., Talbot, K. & Turner, M. R. Integration of structural and functional magnetic resonance imaging in amyotrophic lateral sclerosis. *Brain* **134**, 3470–3479. https://doi.org/10.1093/brain/awr279 (2011).
43. Salimi-Khorshidi, G., Smith, S. M. & Nichols, T. E. Adjusting the effect of nonstationarity in cluster-based and TFCE inference. *Neuroimage* **54**, 2006–2019. https://doi.org/10.1016/j.neuroimage.2010.09.088 (2011).

Acknowledgements

This article is based on a thesis submitted by Seol-Hee Baek for Ph.D. degree at Korea University Graduate School, Seoul, Korea, 2022.

Author contributions

S-H.B. and B-J.K. conducted conceptualization, data acquisition, and data curation. S-H.B. and W-S.T. analyzed the data. S-H.B. wrote the main manuscript text and prepared all figures and tables. D.A. and B-J.K performed the critical revision of the manuscript. All authors reviewed the manuscript. B-J.K. and W-S.T contributed equally to this work as co-corresponding authors.

Funding

None.

Declarations

Competing interests

The authors declare no competing interests.

Additional information

Supplementary Information The online version contains supplementary material available at https://doi.org/10.1038/s41598-025-97666-0.

Correspondence and requests for materials should be addressed to W.-S.T. or B.-J.K.